

# Boron nitride by pyrolysis of the melt-processable poly[tris(methylamino)borane]: Structure, composition and oxidation resistance

Yong-peng Lei <sup>\*</sup>, Ying-de Wang, Yong-cai Song

State Key Lab. of Advanced Ceramic Fibers & Composites, College of Aerospace & Materials Engineering, National University of Defense Technology, Changsha 410073, PR China

Received 5 May 2011; received in revised form 25 June 2011; accepted 2 July 2011

Available online 8th July 2011

## Abstract

Evolution of structure and composition of the melt-processable poly[tris(methylamino)borane] (PTMB) during its conversion to ceramics was studied by TGA, FTIR, Raman, XRD, XPS and elemental analysis (EA). The results show that the ceramic yield was greatly improved from 60.22 to 74.4 wt% at 900 °C by curing in NH<sub>3</sub> prior to pyrolysis. The carbon impurity in the precursor can be removed effectively in NH<sub>3</sub> whereas no similar result occurred in N<sub>2</sub>. In NH<sub>3</sub>, 93 wt% of carbon was removed at 600 °C and the carbon content in the pyrolyzed product at 900 °C was only 0.37 wt%. At the same time, the conversion from polymer to ceramics was almost completed at 900 °C. Moreover, the sample acquired at 900 °C was amorphous boron nitride (BN), while that of further annealing at 1600 °C showed characteristic of turbostratic BN (*t*-BN). Additionally, the BN with nearly stoichiometric composition exhibited good oxidation resistance even up to 900 °C in air.

© 2011 Elsevier Ltd and Techna Group S.r.l. All rights reserved.

**Keywords:** Preceramic polymer; Pyrolysis; Boron nitride; Structure; Oxidation resistance

## 1. Introduction

Nonoxide ceramics derived from preceramic polymers, such as polycarbosilane-derived SiC [1,2], polyborazine-derived BN [3,4] and polyborosilazane-derived SiBN(C) [5,6] have all been researched intensively in recent years. Among them, BN has received great attention as a result of its high chemical stability, low density, excellent oxidation resistance and lubricant characteristic, etc. Nevertheless, it is not easy to fabricate BN with complex shapes using traditional powder sintering and high temperature nitration methods [7,8]. Fortunately, the polymer-derived ceramics (PDCs) route provides a good control of the preceramic polymer's processability to fabricate near-net shapes in a way not known from other techniques [9,10].

Up to date, polymeric precursors to shaped BN were based on borazine [11], B-trichloroborazine [3,12] and (alkylami-

no)borane monomers [13]. As one of the easily synthesized polymeric precursors to BN, poly[tris(methylamino)borane] (PTMB) exhibited great potential in fabricating complex BN devices, such as fibers and coatings [13–19]. As far as we know, though pyrolysis of polyborazene [20] and poly[(alkylamino)-borazine] [21–23] has been widely investigated, that of poly[alkylamino)borane], especially for PTMB, have received less attention. In the present research, evolution of structure and composition of PTMB and anti-oxidation property of BN derived therefrom were studied.

## 2. Experimental

All samples described in this work were manipulated in a dry Ar atmosphere. The PTMB precursor was synthesized as reported previously [13,24], which contains the synthesis of tris(methylamino)borane monomer and followed thermal condensation. In a pyrolysis procedure, the polymer precursor lumps were firstly ground to a fine powder with a diameter less than 20 μm in a glove box, and then cured in NH<sub>3</sub> for a while. After that, the cured powders were weighed into an alumina

<sup>\*</sup> Corresponding author. Tel.: +86 731 84575118; fax: +86 731 84575118.

E-mail addresses: [lypkd@yahoo.com.cn](mailto:lypkd@yahoo.com.cn) (Y.-p. Lei), [wyd502@163.com](mailto:wyd502@163.com) (Y.-d. Wang).

boat and then placed in the pyrolysis tube. After purging the system with Ar for 30 min, the sample was heated to the final temperature (4 °C/min) under flowing anhydrous NH<sub>3</sub> (80 ml/min) with a holding time of 2 h. It was then cooled to room temperature naturally. Moreover, the pyrolysis product obtained at 900 °C was annealed for 1 h at temperatures ranging from 1200 to 1600 °C under flowing Ar (heating rate, 5 °C/min). Spinning of the PTMB was carried out using the hand-drawing technique in a glove-box filled with dry N<sub>2</sub> [1].

Boron content was measured by a chemical titration method. Element contents of N, H and C were checked by Leco TCH-600 N/H/O and Leco CS-600 C/S analyzers. Fourier transform infrared (FTIR) spectra were taken on a Nicolet Avatar 360 spectrophotometer as KBr pellets. The morphology of the fiber was observed using a scanning electron microscope (JSM-6300, JEOL). X-ray diffraction (XRD) patterns were obtained using Siemens D-5005, Cu K $\alpha$  radiation. HRTEM images were obtained using a Philips CM-200 microscope operated at 200 kV. Raman spectroscopy was carried out using a RM 2000 spectrometer with an argon ion laser at an excitation wavelength of 632.8 nm. The XPS spectra were obtained with a VG ESCALAB MKII instrument (Al K $\alpha$  excitation). TGA was carried out in flowing air at a heating rate of 10 °C/min (Netzsch STA 449C).

### 3. Results and discussion

#### 3.1. Characterization and melt-processability of PTMB

Fig. 1 displays the FTIR spectrum of PTMB. The very intense absorption at 1380 cm<sup>-1</sup> and weak absorption at 728 cm<sup>-1</sup> can be assigned to the  $\nu$ (B–N) and  $\delta$ (B–N), respectively [25,26]. Moreover, strong stretching mode of N–H group at 3436 cm<sup>-1</sup>, weak NH<sub>2</sub> bending at 1612 cm<sup>-1</sup> and C–N groups at 1091 cm<sup>-1</sup>, typical bands for C–H bonds in the range of 2930–3090 cm<sup>-1</sup> were also noticed. Table 1 illustrates an overview of the most important FTIR absorptions of PTMB and the sample pyrolyzed at 1600 °C.

Polymer fiber was easily prepared by hand-drawing PTMB in the glove box filled with Ar, as described in the literature

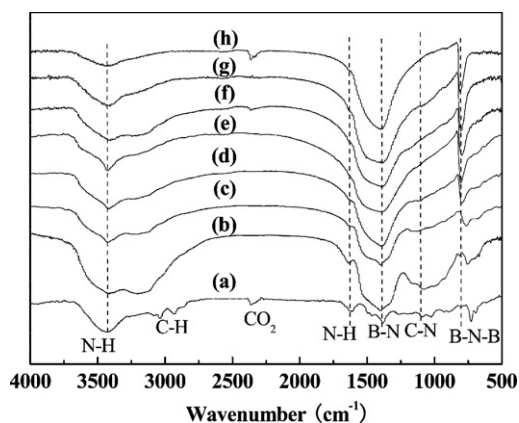


Fig. 1. FTIR spectra of PTMB (a) and PTMB derived sample pyrolyzed at: (b) 400 °C, (c) 600 °C, (d) 800 °C, (e) 900 °C, (f) 1200 °C, (g) 1400 °C and (h) 1600 °C.

Table 1

FTIR absorptions of PTMB and the sample pyrolyzed at 1600 °C.

FTIR bands	Polymer, cm <sup>-1</sup>	Pyrolyzed sample, cm <sup>-1</sup>
$\nu$ (N–H)	3436/1026	
$\delta$ (N–H)	1612	
$\nu$ (C–H)	3081/3037/2929/1493	
$\nu$ (B–N)	1380	1399
$\nu$ (C–N)	1091	
$\delta$ (B–N)	728	810

[27]. The fiber in a diameter of about 20  $\mu$ m exhibited a smooth surface without obvious flaws, as shown in Fig. 2. But even now, just like polycarbosilane fiber [28], the polymer fiber in this study was also very fragile and cannot survive any mechanical shock.

#### 3.2. Conversion from polymer to ceramics

As reported earlier [27], curing in NH<sub>3</sub> could significantly improve the ceramic yield of the polymeric precursor. Here, the pyrolysis behavior of PTMB in NH<sub>3</sub> after curing or not was also examined. Fig. 3 gives the TGA curves of both samples, from which it can be seen that the ceramic yield was different. For the sample without curing, the ceramic yield was 24.07 wt% at 900 °C. While for the sample cured at 80 °C for 10 h, the ceramic yield was enhanced to 38.01 wt%. Moreover, most of the weight loss (98.0 wt% for un-cured and 97.1 wt% for cured, respectively) occurred at 600 °C for both samples. The weight loss between 600 and 900 °C were both less than 3 wt% of the total weight loss at 900 °C.

Prior to curing, the elemental composition (wt%) of PTMB was: B (24.51), C (32.82), N (29.87) and H (10.21), separately, from which the chemical formula was determined to be BC<sub>1.20</sub>N<sub>0.94</sub>H<sub>4.5</sub>. It is worthy to note that the carbon content decreased drastically from 32.82 to 24.85 wt% after curing in NH<sub>3</sub> owing to the release of methylamine during curing, similar to that described by Cornu and coworkers [13].

Fig. 4 shows the evolution of carbon content in cured PTMB as a function of temperature under NH<sub>3</sub>. As seen, with

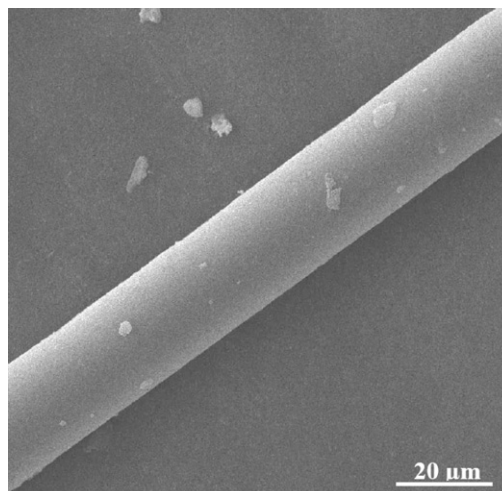


Fig. 2. The typical morphology of the polymer fiber.

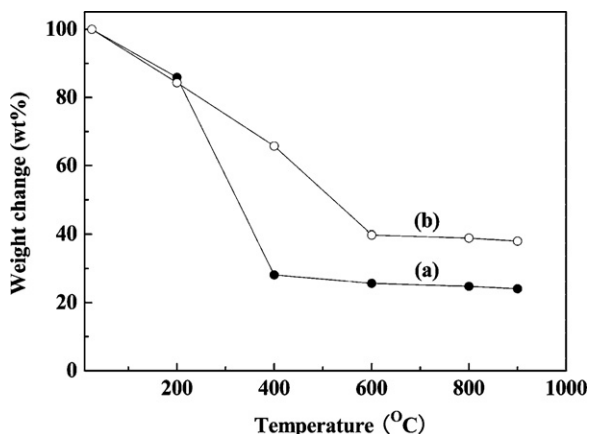
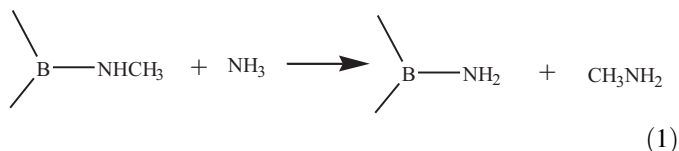


Fig. 3. TGA curves of PTMB in  $\text{NH}_3$ : (a) un-cured and (b) cured at  $80^\circ\text{C}$  for 10 h.

increasing temperature, the carbon content decreased significantly below  $400^\circ\text{C}$  and occupied about 80.3 wt% of the total carbon removal. Moreover, 93 wt% of carbon was removed at  $600^\circ\text{C}$ . When the temperature was elevated to  $800^\circ\text{C}$ , the carbon content reduced much slower and changed from 5.26 to 0.73 wt%. Above  $800^\circ\text{C}$ , there was no obvious reduction in the carbon content and it reached about 0.37 wt% at  $900^\circ\text{C}$ . However, the carbon content in the  $\text{N}_2$  pyrolyzed sample was 5.67 wt% at  $900^\circ\text{C}$ . The difference between two residues was also reflected in the sample color that the former was gray white while the latter was black [29]. The smooth carbon removal in  $\text{NH}_3$  was mainly due to the evolution of methylamine caused by transamination reaction (Eq. (1)) and the carbothermal reaction of carbon with  $\text{NH}_3$  (Eq. (2)), as shown below [13,30].



The evolution of the structure during pyrolysis was analyzed by FTIR spectra, as represented in Fig. 1. With the temperature increasing, the intensity of C–H, N–H and C–N bands

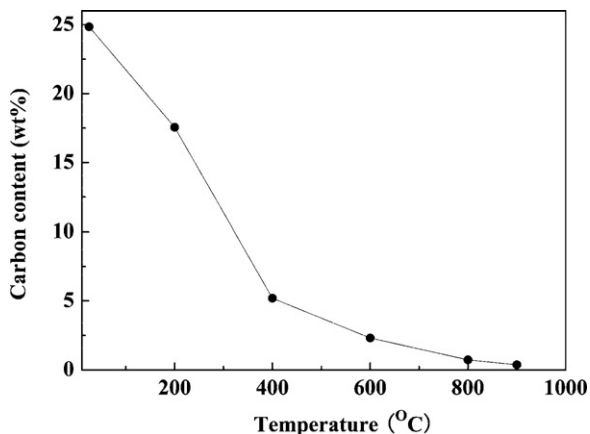


Fig. 4. Evolution of carbon content as a function of temperature.

decreased gradually. The C–H band was almost absent in the sample obtained at  $400^\circ\text{C}$  as a result of elimination of methylamine according to Eq. (1) and the intensity of B–N band increased obviously. Also, the intensity of the C–N band at  $1026\text{ cm}^{-1}$  showed a reduction supplying the decrease of carbon content. The band attributed to N–H group around  $1612\text{ cm}^{-1}$  became weak. Moreover, a wide N–H band corresponding to  $\text{NH}_2$  was also observed at about  $3209\text{ cm}^{-1}$  caused by transamination reaction, as Eq. (1) displayed.

At  $600^\circ\text{C}$ , the N–H band at  $3209\text{ cm}^{-1}$  was not observed and the intensity of C–N band became very weak. Upon further heating up to  $900^\circ\text{C}$ , the C–N band was almost absent, indicating that the carbon content was very low. The result was in consonance with that of EA. Moreover, the FTIR spectrum at  $900^\circ\text{C}$  showed characteristic of BN and those above  $900^\circ\text{C}$  changed little, suggesting that the conversion of polymer to ceramics was almost completed at  $900^\circ\text{C}$ . As the temperature was further increased, the N–H band at around  $3436\text{ cm}^{-1}$  became weaker gradually. The sample annealed at  $1600^\circ\text{C}$  showed  $\nu(\text{B}-\text{N})$  and  $\delta(\text{B}-\text{N})$  vibrations at  $1399$  and  $810\text{ cm}^{-1}$ , respectively, confirming the formation of BN [25,26]. Furthermore, the shift of frequency from polymer to ceramics for  $\delta(\text{B}-\text{N})$  was associated with modification of the atomic environment and the crystallization process [21].

Raman spectra of the PTMB pyrolyzed at various temperatures were presented in Fig. 5. Obviously, the diffuse Raman spectra showed characteristic BN near  $1500\text{ cm}^{-1}$ . As studied by Rye et al. [20], the large width of the band was characteristic of the amorphous BN. The humps shifted to lower wavenumber due to the increase of crystallinity. It is worth noting that a broad diffuse band at around  $2900\text{ cm}^{-1}$  was also present, which was caused by the characteristic of BN overtone. Moreover, there was no emergence of characteristic peak of carbon located around  $1600\text{ cm}^{-1}$  [31], indicating complete removal of carbon. Hence, the result of Raman spectra confirmed that of EA above.

The microstructure evolutions of the BN phases were also confirmed by XRD, as displayed in Fig. 6. From Fig. 6, characteristics of amorphous BN can be observed in the residue acquired at  $800^\circ\text{C}$ , similar to that obtained from  $900$  to  $1400^\circ\text{C}$ . The same shape in XRD patterns indicated very slow crystallization below  $1400^\circ\text{C}$ .

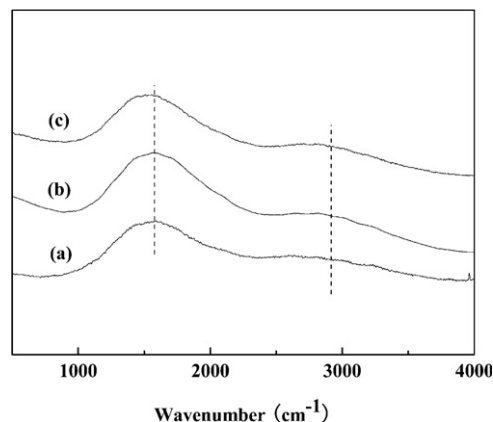


Fig. 5. Raman spectra of PTMB pyrolyzed at various temperatures: (a)  $1200^\circ\text{C}$ , (b)  $1400^\circ\text{C}$  and (c)  $1600^\circ\text{C}$ .

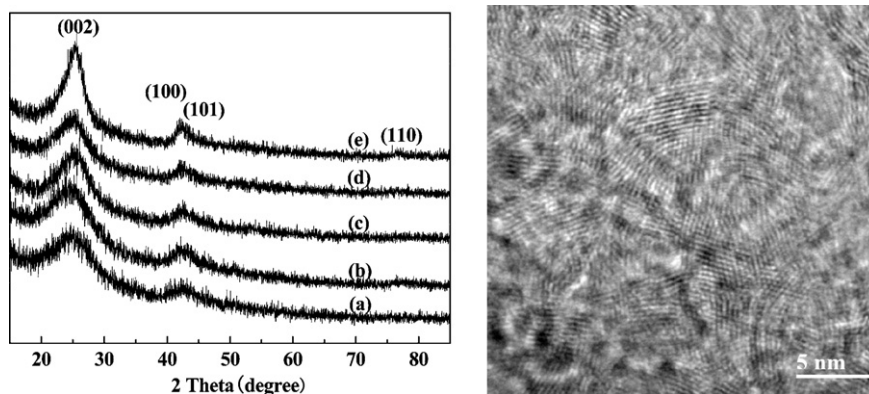


Fig. 6. XRD patterns of the samples obtained at different temperatures: (a) 800 °C, (b) 900 °C, (c) 1200 °C, (d) 1400 °C, (e) 1600 °C and HRTEM image of the sample pyrolyzed at 1600 °C (f).

After heat treated at 1600 °C, the XRD patterns of the sample changed a lot, implying a great phase development happened between 1400 and 1600 °C. Clearly, the full width half maximum (FWHM) of the (0 0 2) plane was narrower compared with that obtained at 800 °C. The sample exhibited no resolution of the (1 0 0) and (1 0 1) plane, showing characteristics of *t*-BN [4,7,22]. Furthermore, a weak peak around  $2\theta = 76^\circ$  was attributed to the (1 1 0) reflection. However, the value of average interlayer spacing of the (0 0 2) plane  $d_{002}$  (0.347 nm) was much higher than that of hexagonal BN (*h*-BN) (0.333 nm) [32], illustrating a lower degree of crystallinity. A higher crystallinity could be acquired by enhancing the pyrolysis temperature [7]. Due to its randomness and partially disordered properties, *t*-BN does not have an accurate crystal structure, and its lattice constants are usually determined by reference to *h*-BN [33]. The lattice

constants of the obtained *t*-BN were  $a = 2.469 \text{ \AA}$  and  $c = 6.975 \text{ \AA}$ , corresponding to the previous research [33,34]. Additionally, a further investigation of the microstructure for the sample revealed partially ordered BN by HRTEM (Fig. 6(f)) [35], in good agreement with the XRD result.

The composition information of the sample pyrolyzed at 1600 °C was investigated by the XPS spectra, as illustrated in Fig. 7. The survey spectrum (Fig. 7(a)) revealed the presence of B and N elements. Small quantity of C and O were also detected probably as a consequence of the absorption of CO<sub>2</sub> and O<sub>2</sub> on the surface of the sample. The split B1s and N1s spectra were shown in Fig. 7(b) and (c), respectively. The B1s peak at 190.5 eV and the N1s peak at 398.0 eV indicated BN [36]. Carbon element was not detected, pointing out a complete removal of carbon impurity during pyrolysis, in consistent with the EA result. Moreover, the N/B atomic ratio

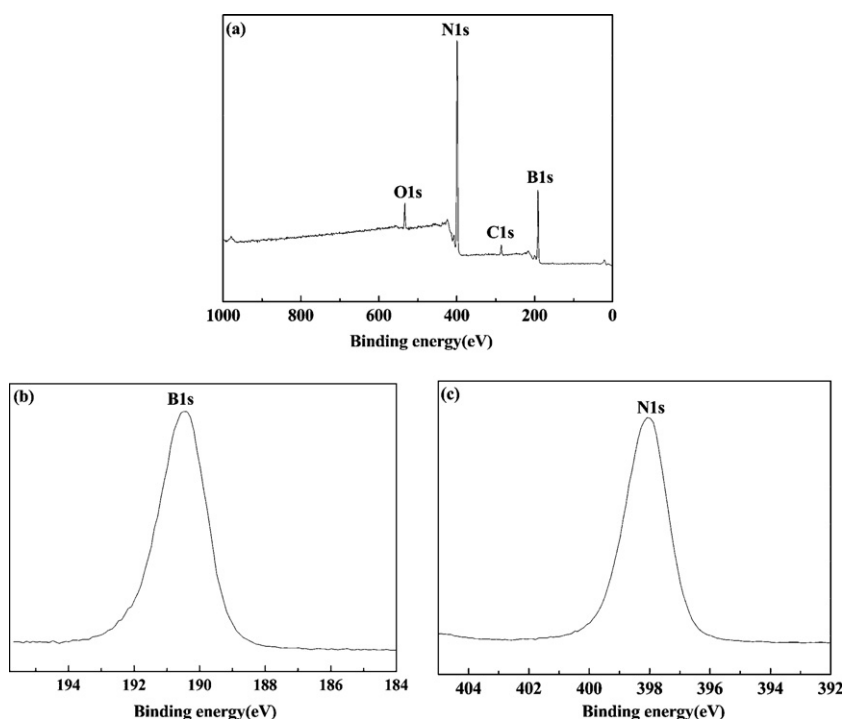


Fig. 7. XPS spectra of the sample obtained at 1600 °C: (a) survey spectra, (b) B1s peak and (c) N1s peak.

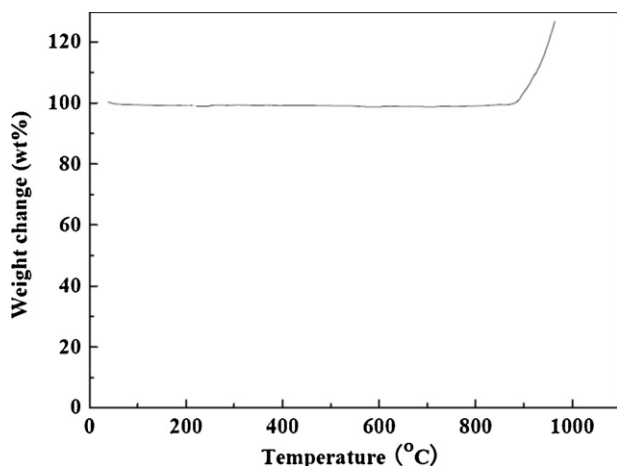


Fig. 8. TGA curve of as-obtained BN heated 10 °C/min in air.

determined by XPS was about 1.00, which was near-stoichiometric, making it possible to possess good oxidation resistance [7].

### 3.3. Oxidation resistance

The high temperature stability of advanced ceramics is important in determining the suitability for their applications, especially used in oxygen-containing environments [7,35,37,38]. Fig. 8 gives the TGA curve of as-prepared BN in air. It can be seen that the sample displayed less than 3.0 wt% weight change up to 900 °C. Clearly, the sample began to gain weight at about 900 °C due to oxidation of BN. In order to better understand the oxidation behavior of as-obtained BN, the isothermal oxidation process of the BN at 950 °C was also researched, as shown in Fig. 9. As seen, the sample exhibited a continual weight gain till about 80 min.

It is known that BN was oxidized to B<sub>2</sub>O<sub>3</sub> when exposed to oxygen/moisture at temperature between 800 and 900 °C, as Eqs. (3) and (4) displayed [39]. The stability to oxidation of BN depends closely on its crystallinity [7,40]. Namely, the BN possessing higher crystallinity exhibits better anti-oxidation property [41,42]. In fact, Cofer and coworkers [41] have tested

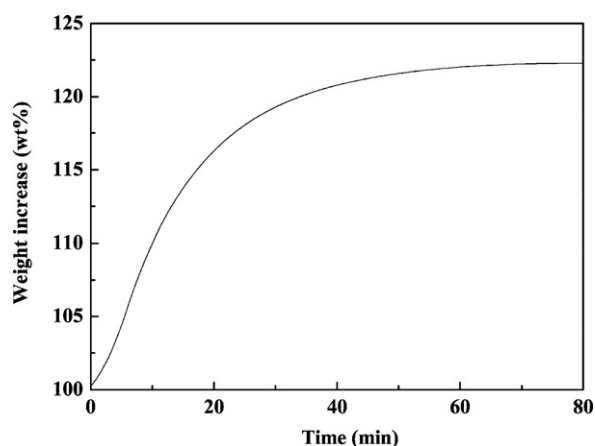
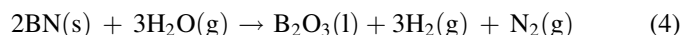
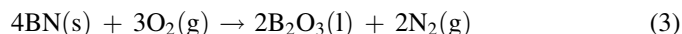


Fig. 9. Isothermal weight gain in air at 950 °C for as-obtained BN (10 °C/min to 950 °C then held).

the oxidation resistance of BN with different crystallinity. They found that BN with  $d_{002}$  of 0.333 nm showed a slower weight gain than those with bigger  $d_{002}$ . Hence, it is possible to improve the oxidation resistance of as-prepared BN by applying higher heat-treated temperature to elevate the crystallinity.



## 4. Conclusions

In conclusion, PTMB precursor for BN showed good processability by melt-spinning it into fiber. The ceramic yield was greatly improved by curing in NH<sub>3</sub>. Pyrolysis under NH<sub>3</sub> led to a complete carbon removal while not under N<sub>2</sub>. Moreover, the structure and composition of pyrolysis intermediates were analyzed by FTIR, Raman and EA, illustrating complete conversion of polymer into ceramics at 900 °C. Furthermore, the sample heat treated at 1600 °C showed characteristics of *t*-BN and a near-stoichiometric composition. In addition, the BN displayed good stability in air even up to 900 °C. Higher oxidation resistance would be obtained by applying higher pyrolysis temperature.

## Acknowledgements

The authors acknowledge the National High technology Research and Development of China (No. 2006AA03A217) for financial support. The authors wish to thank Prof. Y.M. Si for helpful discussion.

## References

- [1] S. Yajima, K. Okamura, M. Hayashi, Continuous silicon carbide fiber of tensile strength, *Chem. Lett.* 68 (1975) 1209–1222.
- [2] Y. Ma, S. Wang, Z.H. Chen, In situ growth of a carbon interphase between carbon fibers and a polycarbosilane-derived silicon carbide matrix, *Carbon* 49 (2011) 2869–2872.
- [3] B. Toury, P. Miele, D. Cornu, H. Vincent, J. Bouix, Boron nitride fibers prepared from symmetric and asymmetric alkylaminoborazines, *Adv. Funct. Mater.* 12 (2002) 228–234.
- [4] U. Kusari, Z. Bao, Y. Cai, G. Ahmad, K.H. Sanhage, L.G. Sneddon, Formation of nanostructured, nanocrystalline boron nitride micro particles with diatom-derived 3D shapes, *Chem. Commun.* 117 (2007) 7–1179.
- [5] Y.H. Sehlleier, A. Verhoeven, M. Jasen, Observation of direct bonds between carbon and nitrogen in Si–B–N–C ceramic after pyrolysis at 1400 °C, *Angew. Chem. Int. Ed.* 47 (2008) 3601–3602.
- [6] Y. Tang, J. Wang, X.D. Li, Z.F. Xie, H. Wang, W.H. Li, X.Z. Wang, Polymer-derived SiBN fiber for high-temperature structural/functional applications, *Chem. Eur. J.* 16 (2010) 6458–6462.
- [7] R.T. Paine, C.K. Narula, Synthetic routes to boron nitride, *Chem. Rev.* 90 (1990) 73–91.
- [8] J. Li, S. Bernad, V. Salles, C. Gervais, P. Miele, Preparation of polyborazylene-derived bulk boron nitride BN with tunable properties by warm-pressing and pressureless pyrolysis, *Chem. Mater.* 22 (2010) 2010–2019.
- [9] P. Colombo, G. Mera, R. Riedel, G.D. Sorarù, Polymer-derived ceramics: 40 years of research and innovation in advanced ceramics, *J. Am. Ceram. Soc.* 93 (2010) 1805–1837.

- [10] H. Termoss, M. Bechelany, B. Toury, A. Brioude, S. Bernard, D. Cornu, P. Miele, Shaping potentialities of aluminum nitride polymeric precursors. Preparation of thin coatings and 1D nanostructures in liquid phase, *J. Eur. Ceram. Soc.* 29 (2009) 857–861.
- [11] T. Wideman, E.E. Remsen, E. Cortez, V.L. Chlanda, L.G. Sneddon, Amine-modified polyborazylens: second-generation precursors to boron nitride, *Chem. Mater.* 10 (1998) 412–421.
- [12] Y.P. Lei, Y.D. Wang, Y.C. Song, C. Deng, Novel processable precursor for BN by the polymer-derived ceramics route, *Ceram. Int.* (2011), doi:10.1016/j.ceramint.2011.04.021.
- [13] D. Cornu, P. Miele, R. Faure, B. Bonnetot, H. Mongeot, J. Bouix, Conversion of  $B(NHCH_3)_3$  into boron nitride and polyborazine fibres and tubular BN structures derived therefrom, *J. Mater. Chem.* 9 (1999) 757–761.
- [14] S.T. Li, Y.M. Cao, K.Q. Han, X. Zhao, M.H. Yu, Precursor based on polyborylborazine for BN fiber: preparation and rheology properties, *J. Macromol. Sci. B* 48 (2009) 1132–1142.
- [15] F. Guilhon, B. Bonnetot, D. Cornu, H. Mongeot, Conversion of tris(isopropylamino)borane to polyborazines. Thermal degradation to boron nitride, *Polyhedron* 15 (1999) 851–859.
- [16] B. Bonnetot, F. Guilhon, J.C. Viala, H. Mongeot, Boron nitride matrices and coatings obtained from tris(methylamino)borane. Application to the protection of graphite against oxidation, *Chem. Mater.* 7 (1995) 299–303.
- [17] F. Thévenot, C. Doche, H. Mongeot, F. Guilhon, P. Miele, D. Cornu, B. Bonnetot, Boron nitride obtained from molecular precursors: aminoboranes used as a BN source for coatings, matrix, and  $Si_3N_4$ -BN composite ceramic preparation, *J. Solid State Chem.* 133 (1997) 164–168.
- [18] C. Doche, F. Guilhon, B. Bonnetot, F. Thevenot, H. Mongeot, Elaboration and characterization of  $Si_3N_4$ -BN composites from tris(methylamino)borane as a boron nitride precursor, *J. Mater. Sci. Lett.* 14 (1995) 847–850.
- [19] F. Thévenot, C. Doche, H. Mongeot, F. Guilhon, P. Miele, B. Bonnetot,  $Si_3N_4$ -BN composites obtained from aminoboranes as BN precursors and sintering aids, *J. Eur. Ceram. Soc.* 17 (1997) 1911–1915.
- [20] R.R. Rye, D.R. Tallant, T.T. Borek, D.A. Lindquist, R.T. Paine, Mechanistic studies of the conversion of borazine polymers to boron nitride, *Chem. Mater.* 3 (1991) 286–293.
- [21] S. Bernard, D. Cornu, P. Miele, H. Vincent, J. Bouix, Pyrolysis of poly[2,4,6-tri(methylamino)borazine] and its conversion into BN fibers, *J. Organomet. Chem.* 657 (2002) 91–97.
- [22] S. Bernard, K. Ayadi, M.P. Berthet, F. Chassagneux, D. Cornu, J.M. Letoffe, P. Miele, Evolution of structural features and mechanical properties during the conversion of poly[(methylamino)borazine] fibers into boron nitride fibers, *J. Solid State Chem.* 177 (2004) 1803–1810.
- [23] S. Duperrier, C. Gervais, S. Bernard, D. Cornu, F. Babonneau, P. Miele, Controlling the chemistry, morphology and structure of boron nitride-based ceramic fibers through a comprehensive mechanistic study of the reactivity of spinnable polymers with ammonia, *J. Mater. Chem.* 16 (2006) 3126–3138.
- [24] D.W. Aubrey, M.F. Lappert, Cyclic organic boron compounds. Part IV. B-amino- and B-alkoxy-borazoles and their precursors the tris(primary amino)borons and (primary amino)boron alkoxides, *J. Chem. Soc.* 19 (1959) 2927–2931.
- [25] L.Q. Xu, Y.Y. Peng, Z.Y. Meng, W.C. Yu, S.Y. Zhang, X.M. Liu, Y.T. Qian, A co-pyrolysis method to boron nitride nanotubes at relative low temperature, *Chem. Mater.* 15 (2003) 2675–2680.
- [26] P. Dibandjo, L. Bois, F. Chassagneux, D. Cornu, J.M. Letoffe, B. Toury, F. Babonneau, P. Miele, Synthesis of boron nitride with ordered mesostructure, *Adv. Mater.* 177 (2005) 571–574.
- [27] Y.P. Lei, Y.D. Wang, Y.C. Song, C. Deng, H. Wang, Nearly stoichiometric BN fiber by curing and thermolysis of a novel poly[(alkylamino)borazine], *Ceram. Int.* 37 (2011) 1795–1800.
- [28] C. Laffon, A.M. Flank, P. Lagarde, M. Laridjani, Study of nicalon-based ceramic fibers and powders by EXAFS spectrometry, X-ray diffractometry and some additional methods, *J. Mater. Sci.* 24 (1989) 1503–1512.
- [29] Y. Tang, J. Wang, X.D. Li, W.H. Li, H. Wang, X.Z. Wang, Thermal stability of polymer derived SiBNC ceramics, *Ceram. Int.* 35 (2009) 2871–2876.
- [30] N.S.C.K. Yive, R.J.P. Corriu, D. Leclercq, P.H. Mutin, A. Vioux, Thermo-gravimetric analysis/mass spectrometry investigation of the thermal conversion of organosilicon precursors into ceramic under argon and ammonia. 2. Poly(silazane), *Chem. Mater.* 4 (1992) 1263–1271.
- [31] Y. Ma, S. Wang, Z.H. Chen, Raman spectroscopy studies of the high-temperature evolution of the free carbon phase in polycarbosilane derived SiC ceramics, *Ceram. Int.* 36 (2010) 2455–2459.
- [32] T. Hagio, K. Nonaka, T. Sato, Microstructural development with crystallization of hexagonal boron nitride, *J. Mater. Sci. Lett.* 16 (1997) 795–798.
- [33] J.B. Lian, T. Kim, X.D. Liu, J.M. Ma, W.J. Zheng, Ionothermal synthesis of turbostratic boron nitride nanoflakes at low temperature, *J. Phys. Chem. C* 113 (2009) 9135–9140.
- [34] A.J.C. Wilson, X-ray diffraction by random layers: ideal line profiles and determination of structure amplitudes from observed line profiles, *Acta Cryst.* 2 (1949) 245–251.
- [35] M.K. Cinibulk, T.A. Parthasarathy, Characterization of oxidized polymer-derived SiBCN fibers, *J. Am. Ceram. Soc.* 84 (2001) 2197–2202.
- [36] H. Vincent, F. Chassagneux, C. Vincent, B. Bonnetot, M.P. Berthet, A. Vuillermoz, J. Bouix, Microtexture and structure of boron nitride fibres by transmission electron microscopy, X-ray diffraction, photoelectron spectroscopy and Raman scattering, *Mater. Sci. Eng. A* 340 (2003) 181–192.
- [37] W.M. Guo, H.N. Xiao, Mechanisms and modeling of oxidation of carbon felt/carbon composites, *Carbon* 45 (2007) 1058–1065.
- [38] Y.G. Wang, H.B. Li, L.T. Zhang, L.F. Cheng, Oxidation behavior of polymer derived SiCO powders, *Ceram. Int.* 35 (2009) 1129–1132.
- [39] N. Jacobson, S. Farmer, A. Moore, H. Sayir, High-temperature oxidation of boron nitride: I, monolithic boron nitride, *J. Am. Ceram. Soc.* 82 (1999) 393–398.
- [40] X.B. Yan, L. Gottardo, S. Bernard, P. Dibandjo, A. Brioude, H. Mou-taabbid, P. Miele, Ordered mesoporous silicoboron carbonitride materials via preceramic polymer nanocasting, *Chem. Mater.* 20 (2008) 6325–6334.
- [41] C.C. Cofer, J. Economy, Oxidation and hydrolytic stability of boron nitride—a new approach to improving the oxidation resistance of carbonaceous structures, *Ceram. Int.* 33 (1995) 389–395.
- [42] V.A. Lavrenko, A.F. Alexeev, High-temperature oxidation of boron nitride, *Ceram. Int.* 12 (1986) 25–31.